Transverse field effect in graphene ribbons

D. S. Novikov

W. I. Fine Theoretical Physics Institute, University of Minnesota, Minneapolis, MN 55455
(Dated: July 31, 2007)

It is shown that a graphene ribbon, a ballistic strip of carbon monolayer, may serve as a quantum wire whose electronic properties can be continuously and reversibly controlled by an externally applied transverse voltage. The electron bands of armchair-edge ribbons undergo dramatic transformations: The Fermi surface fractures, Fermi velocity and effective mass change sign, and excitation gaps are reduced by the transverse field. These effects are manifest in the conductance plateaus, van Hove singularities, thermopower, and activated transport. The control over one-dimensional bands may help enhance effects of electron correlations, and be utilized in device applications.

PACS numbers: 73.23.-b 73.63.-b 72.80.Rj

Building nanoscale systems with pre-determined properties has long been the focus of basic and applied research. Progress in this field is tied to the recent advancements in the synthesis of quantum nanowires [1] and quantum dots [2] via control of the growth process, as well as in the growth and selection of carbon nanotubes [3]. The characteristics of these devices, however, are set by design and are typically difficult to modify. Ideally, one would like to be able to tune the system's properties reversibly after synthesis.

In the present work we suggest that a graphene ribbon (GR), a ballistic strip of recently discovered [4] carbon monolayer, may serve as a quantum wire whose electronic properties can be continuously and reversibly controlled by the external transverse voltage. The setup makes use of the massless relativistic electron dispersion in graphene [4–6], with the valence and conduction bands touching at a conical Dirac point [3, 7].

Electron dispersion in GRs varies depending on their chirality, as the transverse confinement of Dirac fermions is sensitive to the boundary conditions [8–16]. This has prompted proposals for GR applications as field-effect transistiors [17] and valley filters [18]. Furthermore, GRs have been suggested as a host of interesting many-body phenomena, including spin polarization on the edges [19, 20], and as a basis for building coupled electron spin qubits [21]. Recently spectral gaps in GRs have been measured [22], scaling approximately inversely with the ribbon width.

The basic idea of the present proposal is that the properties at the Dirac point are fragile and can be affected by external fields [23]. Not suprisingly, the proposed strong electric field effect is similar to that considered for carbon nanotubes [24–26]. Unfortunately, small radius $R \sim 1$ nm of single-walled tubes requires very large transverse fields $\mathcal{E}_{[\mathrm{MV/cm}]} \simeq 25/R_{[\mathrm{nm}]}^2$; this has so far hindered observation of band transformation. Remarkably, with GRs, the ribbon width (that plays the role of the tube circumference) may vary in a broad range, $L \sim 10-200$ nm [22], and the effects of strong band transformation become realistic.

In the setup shown in Fig. 1, electrons in a GR are con-

fined along the x axis, while the longitudinal momentum $k_y \equiv k$ is conserved. The effect of the applied transverse voltage V is to induce the potential

$$U(x) = -e\mathcal{E}(x - L/2). \tag{1}$$

The acting field $\mathcal{E} \propto \mathcal{E}_{\mathrm{ext}} \propto V$ can be assumed uniform and proportional to the external field $\mathcal{E}_{\mathrm{ext}}$ as long as the bands are not strongly mixed (as described below); e is the unit charge. We subtracted the average, setting $\int_0^L dx\, U(x) = 0$ (the subtracted constant adds to the chemical potential controlled by the gate voltage V_g). The natural units for the transverse voltage and energy

$$u = e\mathcal{E}L/\Delta_L, \quad \Delta_L = \hbar v/L \simeq 0.7\,\mathrm{eV}/L_{[\mathrm{nm}]}, \tag{2}$$

where $v \simeq 10^6$ m/s is graphene's Fermi velocity. The ballistic limit of transport is implied.

We now give an overview of the results. The electron band transformation is shown in Figs. 2 and 3. The longitudinal electron bands change qualitatively when the
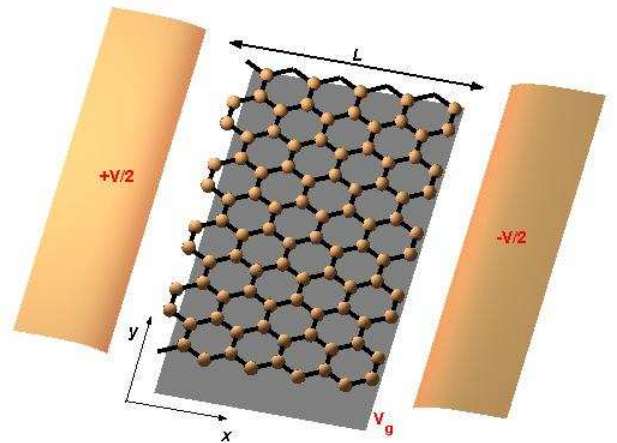

FIG. 1: (color online). The setup. Left and right electrodes carry the voltage $\pm V/2$, producing the external field $\mathcal{E}_{\mathrm{ext}}$. The carrier concentration is controlled by the back gate voltage V_g.
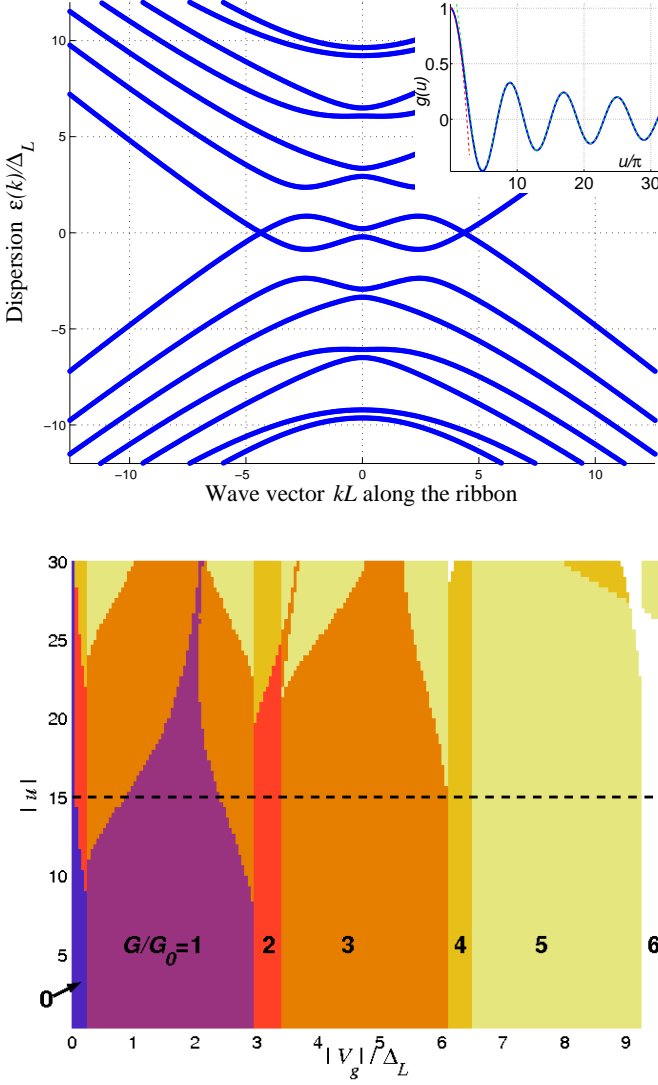
FIG. 2: (color online). Transverse field effect in metallic GRs. *Inset:* Velocity reversals in metallic GRs occur at the zeros of the function $g(u)$, Eq. (9); first reversal voltage $u_1 \approx 9.2$. Fine lines show the $u \ll 1$ and $u \gg 1$ asymptotic behavior of $g(u)$. *Top:* The voltage $u = 15$ above the reversal value u_1. The Fermi surface acquires a pair of small pockets. Small gaps at $k = 0$ are due to imperfect boundaries [20]. *Bottom:* Landauer conductance G (bold integers and colors) in the units of $G_0 = 2e^2/h$, as the number of transverse modes at the Fermi energy V_g. Dashed cut corresponds to the top panel.
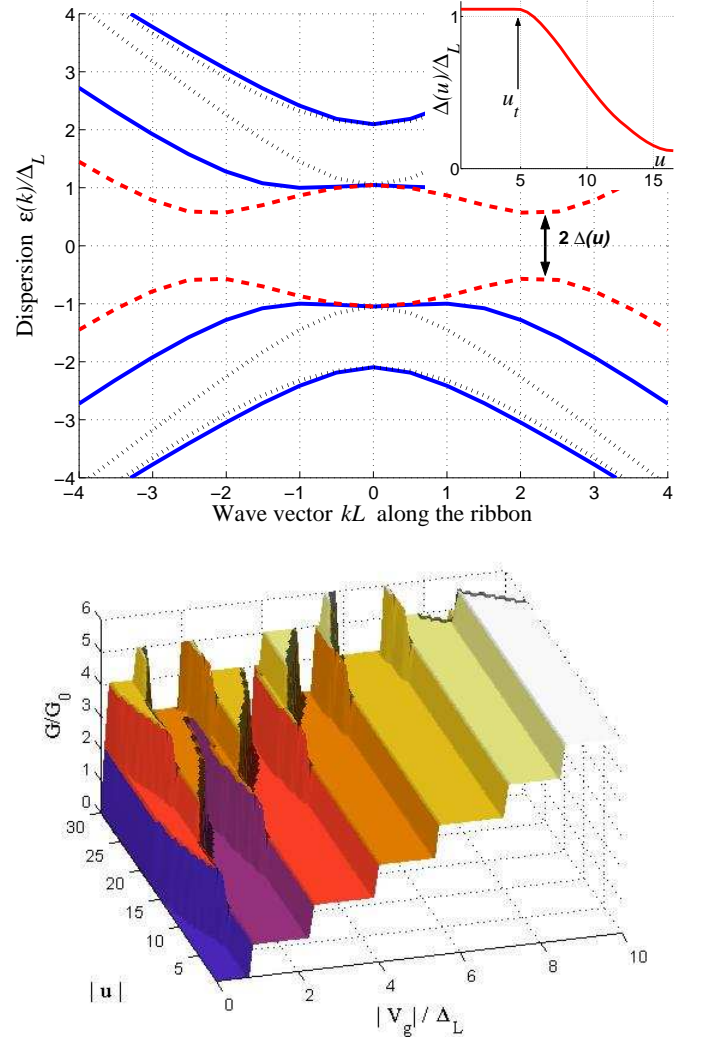

FIG. 3: (color online). Transverse field effect in semiconducting GRs. For voltages $u > u_t \approx 4.5$ above threshold the effective mass at $k = 0$ is negative. *Top:* Bands transformation, starting from $u = 0$ (dotted), to just above threshold $u = 6$ (solid), to above threshold, $u = 10$ (dashed, only lowest subbands shown), where the gap is minimal at $k \neq 0$. *Inset:* Gap suppression occurs above the threshold u_t. *Bottom:* Landauer conductance plateaus in the units of $G_0 = 2e^2/h$.

dimensionless transverse voltage approaches $u \sim 10$. A number of effects follow:

(i) The Landauer conductance [27] is quantized in the units of $G_0 = 2e^2/h$, similar to that in point contacts in GaAs [28]. The crucial difference is that now the positions and widths of the plateaus can be controlled by the transverse voltage. The sharp steps in Figs. 2 and 3 in real systems will be smoothened out by finite temperature or weak disorder, while the conductance values on the plateaus will remain equal to the quantized values.

(ii) The thermopower $S \propto -\partial \ln G/\partial V_g$, being proportional to the conductance derivative [29], peaks at the borders between the domains in Figs. 2 and 3 (bottom).

(iii) The Fermi velocity in metallic GRs is reduced by the field, $v \to vg(u)$ [Fig. 2 inset and Eq. (9) below]. As a consequence, the one-dimensional density of states at the band center $\nu(0) = 2/\{\pi\hbar v|g(u)|\}$ increases [factor 2 is due to spin degeneracy]. This increase magnifies the effects of electron interactions. The latter may manifest themselves via the increase of the Luttinger liquid exponent in a sufficiently long ribbon, and through excitonic instabilities (resulting in interaction-induced gaps).

(iv) The Fermi velocity changes sign for the field values corresponding to zeroes of $g(u)$, causing strong van Hove singularities in metallic GRs. The Fermi surface fractures, with each sign change adding a pair of small pockets to the Fermi surface (Fig. 2, top). This effect produces extra conductance plateaus (Fig. 2, bottom).

(v) There is a threshold voltage $u_t \simeq 4.5$ above which the effective mass of the lowest energy subband in semiconducting GRs changes sign, so that the longitudinal electron dispersion acquires symmetric minima at small but nonzero k (Fig. 3). The excitation gap is then reduced by the field (Fig. 3 inset). This effect can be detected in the shift of the conductance plateaus (Fig. 3, bottom), and in the activated transport measurements.

(vi) The band structure remains electron-hole symmetric at any field for both metallic and semiconducting GRs due to the Dirac symmetry of the problem. Thus the conductance plots of Figs. 2 and 3 are independent of the polarity of the gate and transverse voltages.

Turning to possible applications, the setup may serve as a field-effect transistor with a tunable working point, in which the "transverse", V, and the "normal", V_g, field effects can be utilized separately. Furthermore, one may selectively amplify combinations $\alpha(V - V^0) + \beta(V_g - V_g^0)$, $\alpha = \partial G / \partial V |_{\mathcal{V}}$ and $\beta = \partial G / \partial V_g |_{\mathcal{V}}$ by choosing an appropriate working point $\mathcal{V} = (V^0, V_g^0)$ on the edge of the conductance plateau. Tuning the parameters to achieve a large gain for say, $V - V_g$, combined with the device's large input and low output impedance, is reminiscent of an operational amplifier. By the same token, strong conductance nonlinearity in both inputs V and V_g may render this setup into a few-nm size signal multiplier, or even into a logic gate.

We now outline the details of the calculation. At the π-band center ($\epsilon = 0$), the electron dispersion is determined by the two inequivalent Dirac points in the Brillouin zone. The low-energy states $\Psi(\mathbf{r}) = e^{iKx}\psi_+(\mathbf{r}) + e^{-iKx}\psi_-(\mathbf{r})$ are represented [3] in terms of the smoothly varying envelope $\psi = \{\psi_+, \psi_-\}$ that consists of the pair of the two-component spinors ψ_+ and ψ_- with values on the two sublattices of the honeycomb lattice [here $K = -4\pi/3a_0$, where $a_0 = \sqrt{3}a_{cc}$ is the graphene lattice constant, and $a_{cc} = 0.144\,\mathrm{nm}$ is the Carbon bond length]. The dynamics of the envelope is governed by the Dirac equation $\mathcal{H}\psi = \epsilon\psi$, with the effective Hamiltonian

$$\mathcal{H} = \begin{pmatrix} \mathcal{H}_+ & 0 \\ 0 & \mathcal{H}_- \end{pmatrix}, \quad \mathcal{H}_\pm = \pm i\hbar v \sigma_1 \partial_x - \hbar v k \sigma_2 + U(x),$$
(3)

where $\sigma_{1,2}$ are the Pauli matrices. The boundary conditions $\Psi(\mathbf{r})|_{x=0,L} = 0$ at the armchair edges dictate [14]

$$\psi_+(0) + \psi_-(0) = 0, \quad \psi_+(L) + e^{i\phi_n}\psi_-(L) = 0, \quad (4)$$

where the phase $\phi_n = KL = -\frac{2\pi}{3}(n + 1 - \delta)$, and $L = \frac{1}{2}(n + 1 - \delta)a_0$ is the effective ribbon width (the distance between the sites on which Ψ vanishes). The phase

ϕ_n may incorporate corrections coming from imperfect edges, similar to the curvature-induced corrections in nanotubes [30]. (For example, the $\delta t/t \approx 0.12$ change in the hopping amplitude at the edges due to the passivated bonds [20] reduces the effective width L and the boundary phase ϕ_n by the amount $\propto \delta = \frac{3\sqrt{3}}{\pi}\frac{\delta t}{t} \approx 0.20$.)

The system (3) and (4) is solved numerically (Figs. 2 and 3) via the transfer matrix approach similar to that of Refs. [24, 25, 31]. Eq. (3) is equivalent to

$$\partial_x \psi_\pm = \pm \mathcal{P}\psi_\pm, \quad \mathcal{P}(x) = k\sigma_3 + i\sigma_1(U - \epsilon)/\hbar v. \quad (5)$$

The armchair boundary conditions (4) require $\mathrm{tr}\,(\mathcal{S}\widetilde{\mathcal{S}}) = 2\cos\phi_n$ for the product of the transfer matrices

$$\mathcal{S} = \mathcal{T}_x e^{\int_0^L \mathcal{P}(x)dx}, \quad \widetilde{\mathcal{S}} = \widetilde{\mathcal{T}}_x e^{\int_0^L \mathcal{P}(x)dx}, \quad (6)$$

where $\mathcal{T}_x$ and $\widetilde{\mathcal{T}}_x$ symbolize the "chronological" and "anti-chronological" orderings of the operators $\mathcal{P}(x)$ that do not commute for different x.

In the absence of the field, the GR spectrum consists of one-dimensional Dirac bands with $|\epsilon_{k=0}| = \Delta_L \times \frac{\pi}{3}|n+1-3p-\delta|$, $p = 0, \pm 1, \pm 2, \ldots$. Thus GRs with $n = 3p - 1$ are metallic (with small gap $\propto \delta$ originating from imperfect boundaries [20]), in which case the lowest energy mode is non-degenerate, and the rest are doubly-degenerate (the latter degeneracy is lifted by the finite δ). The ribbons with $n = 3p$ and $n = 3p - 2$ are semiconducting, with non-degenerate bands, and excitation gaps $|\epsilon_{k=0}| = \Delta_L \times \frac{\pi}{3}(1 \mp \delta)$ correspondingly.

To study the transverse field effect it is convenient to employ the chiral gauge transformation [24, 25]

$$\psi_\pm = e^{\pm i\sigma_1\varphi(x)}\widetilde{\psi}_\pm, \quad \varphi = \int_0^x U(x')dx'/\hbar v, \quad (7)$$

that preserves the boundary conditions (4) and transforms the system (3), $\mathcal{H}_\pm \to \widetilde{\mathcal{H}}_\pm$,

$$\widetilde{\mathcal{H}}_\pm = \hbar v \left[-k\sigma_2 e^{\pm 2i\sigma_1\varphi(x)} \pm i\sigma_1\partial_x \right]. \quad (8)$$

The transformation (7) shows that the spectrum at $k = 0$ is unaffected by the field. For the metallic GRs with ideal edges ($e^{i\phi_n} \equiv 1$), the two degenerate $k = 0$, $\epsilon = 0$ eigenstates, each consisting of a pair $\{\widetilde{\psi}_+, \widetilde{\psi}_-\}$, are

$$|1\rangle = \frac{1}{2}\left\{ \begin{pmatrix} 1 \\ 1 \end{pmatrix}, \begin{pmatrix} -1 \\ -1 \end{pmatrix} \right\} \text{ and } |2\rangle = \frac{1}{2}\left\{ \begin{pmatrix} 1 \\ -1 \end{pmatrix}, \begin{pmatrix} -1 \\ 1 \end{pmatrix} \right\}.$$

Projecting the Hamiltonian (8) onto these states, $\widetilde{\mathcal{H}} \to \hbar v k g(u)\sigma_2$, we find the spectrum around $k = 0$

$$\epsilon = \pm\hbar v|kg(u)|, \quad g = \int_0^1 d\xi \cos[u\xi(1 - \xi)]. \quad (9)$$

The function $g(u)$ is plotted in Fig. 2 inset. For $|u| \ll 1$, $g \simeq 1 - u^2/60$. Its $|u| \gg 1$ form $g \simeq \sqrt{\pi/|u|}\cos[(|u| -$

$\pi)/4]$ determines the successive voltages $u_n \approx \pm(3+4n)\pi$, $n = 0, 1, 2, ...$, where the $k = 0$ velocity changes sign. At those voltages the dispersion $\epsilon \sim k^3$ at $k = 0$, causing the van Hove singularity $\nu(\epsilon) \sim |\epsilon|^{-2/3}$ in the density of states at $\epsilon = 0$, and an additional pair of pockets of Fermi surface emerges. In the $|u| \gg 1$ limit, such pockets appear at the zeroes of g for both metallic and semiconducting GRs.

Electron interactions in graphene result in the RPA screening of the external field $\mathcal{E}_{\text{ext}}$. The screening is scale-invariant, $\mathcal{E} = \mathcal{E}_{\text{ext}}/\kappa$, for an infinite sheet [32], $\kappa = 1 + 2\pi e^2/4\hbar v \simeq 5$. The depolarization problem in nanotubes [24–26, 33–36] also yields $\kappa \simeq 5$ practically independent of the tube radius and chirality. This linear-screening estimate will remain valid in GRs as long as the subbands are not strongly mixed. In the opposite case the field on the ribbon edges, estimated in the Thomas-Fermi fashion, develops an algebraic singularity [37], which corresponds to filling the Fermi-surface pockets. As a result, the uniform field model (1) is justified for weak to moderate fields. For the acting field $u = 10$, the required external field $u_{\text{ext}} \simeq 50$ is achieved at $\mathcal{E}_{\text{ext}} L \simeq 1 \, \text{V}$ across the ribbon width $L = 30 \, \text{nm}$.

To conclude, the transverse voltage applied across a graphene nanoribbon dramatically affects its longitudinal electronic dispersion. The Fermi surface breaks up into pockets for the metallic ribbons, and the excitation gap closes for the semiconducting ones. The strong field effect can lead to interesting physical phenomena as well as be utilized in carbon-based electronic devices.

[1] X. Duan and C. M. Lieber, Adv. Mater. **12**, 298 (2000).
[2] C. B. Murray, C. R. Kagan, and M. G. Bawendi, Annu. Rev. Mater. Sci. **30**, 545-610 (2000).
[3] M.S. Dresselhaus, G. Dresselhaus, Ph. Avouris, *Carbon Nanotubes: Synthesis, Structure, Properties and Applications* (Springer, New York, 2001).
[4] K.S. Novoselov *et al.*, Science **306**, 666 (2004); Nature **438**, 197 (2005).
[5] C. Berger *et al.*, J. Phys. Chem. B **108**, 19912 (2004).
[6] Y. Zhang, J. P. Small, M. E. S. Amori, and P. Kim, Phys. Rev. Lett. **94**, 176803 (2005).
[7] P. R. Wallace, Phys. Rev. **71**, 622 - 634 (1947).
[8] K. Nakada, M. Fujita, G. Dresselhaus, and M. S. Dresselhaus, Phys. Rev. B **54**, 17954 (1996).
[9] M. Fujita, K. Wakabayashi, K. Nakada, and K. Kusakabe, J. Phys. Soc. Jpn. **65**, 1920 (1996).
[10] K. Wakabayashi and T. Aoki, Int. J. Mod. Phys. B **16**, 4897-4909 (2002).
[11] S. Ryu and Y. Hatsugai, Phys. Rev. Lett. **89**, 077002 (2002).
[12] M. Ezawa, Phys. Rev. B **73**, 045432 (2006).
[13] N. M. R. Peres, F. Guinea, and A. H. Castro Neto, Phys. Rev. B **73**, 125411 (2006).
[14] L. Brey and H. A. Fertig, Phys. Rev. B **73**, 195408 (2006); Phys. Rev. B **73**, 235411 (2006).
[15] V. Barone, O. Hod, and G. E. Scuseria, Nano Lett. **6**, 2748 (2006).
[16] P. G. Silvestrov and K. B. Efetov, Phys. Rev. Lett. **98**, 016802 (2007).
[17] B. Obradovic, R. Kotlyar, F. Heinz, P. Matagne, T. Rakshit, M. D. Giles, M. A. Stettler, and D. E. Nikonov, Appl. Phys. Lett. **88**, 142102 (2006); Y. Ouyang, Y. Yoon, J. K. Fodor, and J. Guo, Appl. Phys. Lett. **89**, 203107 (2006).
[18] A. Rycerz, J. Tworzdlo, and C. W. J. Beenakker, Nature Physics **3**, 172 (2007).
[19] Y.-W. Son, M. L. Cohen, and S. G. Louie, Nature **444**, 347 (2006).
[20] Y.-W. Son, M. L. Cohen, and S. G. Louie, Phys. Rev. Lett. **97**, 216803 (2006).
[21] B. Trauzettel, D. V. Bulaev, D. Loss, and G. Burkard, Nature Physics **3**, 192 (2007).
[22] Z. Chen, Y.-M. Lin, M. J. Rooks, and P. Avouris, cond-mat/0701599 (2007); M. Y. Han, B. Oezyilmaz, Y. Zhang, and P. Kim, Phys. Rev. Lett. **98**, 206805 (2007).
[23] Effect of strong transverse field on Landau levels in graphene has been studied by V. Lukose, R. Shankar, and G. Baskaran, Phys. Rev. Lett. **98**, 116802 (2007).
[24] D. S. Novikov and L. S. Levitov, preprint arXiv.org/cond-mat/0204499 (2002); also in B. Altshuler, A. Tagliacozzo and V. Tognetti (Eds.), *Quantum Phenomena in Mesoscopic Systems* (IOS Press, Amsterdam, 2003).
[25] D. S. Novikov and L. S. Levitov, Phys. Rev. Lett. **96**, 036402 (2006).
[26] Y. Li, S. V. Rotkin, and U. Ravaioli, Nano Lett. **3**, 183 (2003).
[27] M. Buttiker, Y. Imry, R. Landauer and S. Pinhas, Phys. Rev. B **31**, 6207 (1985).
[28] B. J. van Wees *et al.*, Phys. Rev. Lett. **60**, 848 - 850 (1988); D. A. Wharam *et al.*, J. Phys. C **21**, L209-L214 (1988).
[29] L. W. Molenkamp, H. van Houten, C. W. J. Beenakker, R. Eppenga, and C. T. Foxon, Phys. Rev. Lett. **65**, 1052 (1990); L. W. Molenkamp, Th. Gravier, H. van Houten, O. J. A. Buijk, M. A. A. Mabesoone, and C. T. Foxon, Phys. Rev. Lett. **68**, 3765 (1992).
[30] C. L. Kane and E. J. Mele, Phys. Rev. Lett. **78**, 1932 (1997).
[31] H.-W. Lee and D. S. Novikov, Phys. Rev. B **68**, 155402 (2003).
[32] J. Gonzalez, F. Guinea, and M. A. H. Vozmediano, Phys. Rev. B **59**, R2474 (1999); D. T. Son, preprint arXiv.org/cond-mat/0701501 (2007).
[33] L. X. Benedict, S. G. Louie, and M. L. Cohen, Phys. Rev. B **52**, 8541 (1995).
[34] M. Krcmar, W. M. Saslow, and A. Zangwill, J. Appl. Phys. **93**, 3495 (2003).
[35] E. N. Brothers, K. N. Kudin, G. E. Scuseria, and C. W. Bauschlicher, Jr., Phys. Rev. B **72**, 033402 (2005).
[36] B. Kozinsky and N. Marzari, Phys. Rev. Lett. **96**, 166801 (2006).
[37] D. B. Chklovskii, B. I. Shklovskii, and L. I. Glazman, Phys. Rev. B **46**, 4026 (1992).